Electroreceptor Model of Weakly Electric Fish *Gnathonemus petersii*: II. Cellular Origin of Inverse Waveform Tuning

Jianwei Shuai,* Yoshiki Kashimori,* Osamu Hoshino,* Takeshi Kambara,* and Gerhard von der Emde#
*Department of Applied Physics and Chemistry, The University of Electro-Communications, Chofu, Tokyo 182-8585, Japan, and #Institute für Zoologie, Universität Bonn, D-53115 Bonn, Germany

ABSTRACT In part I (Shuai et al. 1998. *Biophys. J.* 75:1712–1726), we presented a cellular model of the A- and B-electroreceptors of the weakly electric fish *Gnathonemus petersii.* The model made clear the cellular origin of the differences in the response functions of A- and B-receptors, which sensitively code the intensity of the fish's own electric organ discharge (EOD) and the variations in the EOD waveform, respectively. The main purpose of the present paper is to clarify the cellular origin of the inverse waveform tuning of the B-receptors by using the receptor model. Inverse waveform tuning means that B-receptors respond more sensitively to the 180° inverted EOD than to undistorted or less distorted EODs. We investigated how the A- and B-receptor models respond to EODs with various waveforms, which are the phase-shifted EODs, whose shift angle is varied from $-1°$ to $-180°$, and single-period sine wave stimuli of various frequencies. We show that the tuning properties of the B-receptors arise mainly from the combination of two attributes: 1) The waveform of the stimuli (B_{stim}) effectively sensed by the B-receptor cells. This consists of a first smaller and a second larger positive peak, even though in the original phase-shifted EOD stimuli, the amplitudes of the two positive peaks are reversed. 2) The effective time constant of dynamical response of the receptor cells. It is on the order of the duration of a single EOD pulse. We also calculated the response properties of the A- and B-receptor models when stimulated with natural EODs distorted by various capacitive and resistive objects. Furthermore, we investigated the effect of EOD amplitude on the receptor responses to capacitive and resistive objects. The models presented can systematically reproduce the experimentally observed response properties of natural A- and B-receptor cells. The mechanism producing these properties can be reasonably explained by the variation in the stimulus waveforms effectively sensed by the A- and B-receptor cells and by time constants.

INTRODUCTION

Mormyromast electroreceptor organs, containing A- and B-receptor cells, in the weakly electric fish *Gnathonemus petersii* are employed to sense self-emitted electric organ discharge (EOD) for the purpose of active electrolocation (Bennet, 1965; Szabo and Hagiwara, 1967; Bell, 1990a,b). During active electrolocation, each EOD builds up a three-dimensional electric field around the fish, which can be distorted by objects. The electroreceptor organs of the fish sense the current distortions generated by an object and thus perceive the object-induced field distortions. Animate objects like other fishes, plants, or insect larvae have a complex impedance consisting of a resistive or capacitive component. Capacitive objects cause alterations of the waveform of the local EOD, owing to a frequency-dependent amplitude attenuation and a phase shift of the EOD (Heiligenberg, 1973; Bastian, 1986; von der Emde, 1990; von der Emde and Ronacher, 1994). Recent experiments have shown that the mormyromast input is sufficient for the fish to discriminate between capacitive and resistive objects during electrolocation (von der Emde, 1990; von der Emde and Bleckmann, 1992a,b, 1997; von der Emde and Bell, 1994). In addition, fish can discriminate between objects of different capacitive values (von der Emde, 1990, 1993).

A-receptors are pure amplitude coders (Bell, 1990a,b; von der Emde and Bleckmann, 1992a,b, 1997), whereas B-receptors are, in addition, extremely sensitive to EOD waveform distortions, which are only evoked by objects with capacitive electric properties (von der Emde, 1990). The afferent fibers that innervate electroreceptor organs fire a burst of action potentials to each EOD stimulus. Spike latencies and number of spikes per burst are used to encode EOD amplitude and/or EOD waveform distortions (Szabo and Hagiwara, 1967; Bell, 1990a,b; von der Emde and Bleckmann, 1992b; Hall et al., 1995). A- and B-afferent fibers respond similarly with respect to stimulus amplitude changes, such that as the amplitude is increased, the number of spikes increases and spike latencies are shortened. However, the responses induced by the EOD waveform distortions are quite different between A- and B-afferent fibers. In contrast to A-fibers, B-fibers are extremely sensitive to the waveform distortions of an EOD stimulus. B-afferent fibers respond to waveform distorted EODs with larger number of spikes and shorter spike latencies than to undistorted EODs, even if EOD amplitude has been kept constant (von der Emde and Bleckmann, 1992a,b, 1997). B-cells are therefore said to be "inversely waveform tuned." Von der Emde and Bleckmann (1997) obtained waveform tuning curves for A-

Received for publication 13 November 1998 and in final form 6 March 1999.

Address reprint requests to Dr. Yoshiki Kashimori, Department of Applied Physics and Chemistry, The University of Electro-Communication, Chofu, Tokyo 182-8585, Japan. Tel.: +81-424-43-5470; Fax: +81-424-89-9748; E-mail: kashi@nerve.pc.uec.ac.jp.

Dr. Shuai's present address is Department of Biomedical Engineering, Applied Neural Control Laboratory, Case Western Reserve University, Cleveland, OH 44106.

© 1999 by the Biophysical Society

0006-3495/99/06/3012/14 $2.00

and B-receptor cells that revealed a sharp inverse tuning of B-cells to EOD waveform and a much broader waveform tuning of A-cells. This property of B-receptor systems is essentially important for the fish to recognize objects based on the detection and analysis of minute distortions of the local EOD waveform. However, the cellular origin of the inverse waveform tuning is not yet clear.

The main purpose of the present paper is to clarify the cellular origin of the inversely tuning property of the A- and B-receptor systems by using the electroreceptor model of A- and B-receptors described in the previous paper (Shuai et al., 1998). Using the model, we have shown that the functional differences between A- and B-receptor cells come essentially from the different cell morphologies, as well as from different conductances of the leak ion channels of the apical membranes, and from the different capacitances of the cells (Shuai et al., 1998). As a result, A-cells respond sensitively to EOD intensity, whereas B-cells are additionally sensitive to variations in the EOD waveform.

In the present paper, we investigated in detail how the A- and B-receptor models respond to natural EOD waveform distortion and to phase-shifted EODs (von der Emde and Bleckmann, 1997). We show that the inverse tuning properties of the B-receptors arise mainly from the combination of two properties: 1) The waveform of the stimuli (B_{stim}) effectively sensed by the B-receptor cells is composed mainly of a first relatively small and a second relatively large positive peak, as shown in Fig. 5. In contrast, in the original EOD stimuli (V_{stim}), the first positive peak is larger than the second positive peak (Fig. 2*A*). 2) The effective time constant of dynamical response of the receptor cells is on the order of the time duration of a single EOD pulse. As the waveform distortion of the original EOD stimuli is increased, the second positive peak of the EOD becomes larger, while the first peak becomes smaller (Fig. 2 *B*). This tendency corresponds to the situation in the effective stimuli (B_{stim}) sensed by the B-cells. However, if the temporal range (time constant) of dynamical response of the receptor cells is noticeably shorter than the temporal width of the EOD pulse, the second peak on the potential variation of the cells cannot contribute to the receptor response.

To clarify the response properties of the A- and B-receptor models with respect to the time constants of their dynamical responses, we investigated the responses of the models when they were stimulated with a single sine wave pulse of various frequencies, where the duration of the pulse was varied inversely with its frequency.

Furthermore, to examine the plausibility of the models and of the conclusion based on the models, we calculated the response properties of the models when stimulated with natural EODs distorted by various capacitive and resistive objects, besides the phase-shifted EODs and the single-period sine wave stimuli. We compared our results with experimental results obtained by Bell (1990b) and von der Emde and Bleckmann (1992b, 1997). Our models can reliably reproduce the response properties of natural A- and B-receptors observed experimentally when stimulated with various kinds of natural and computer-generated EOD stimuli.

With the model, we also investigated how the responses of the receptors to the capacitive-distorted EODs are influenced by different EOD amplitudes, because natural objects usually have complex impedances consisting of various combinations of resistance and capacitance.

MODELS

Description of A- and B-receptor models

To get by without making too many references to the previous paper (Shuai et al., 1998), we described briefly the essential parts of the models of A- and B-receptors, which function as an amplitude coder and a waveform distortion coder, respectively. The receptor model consists of a receptor cell and an afferent nerve fiber. The receptor cell membrane is separated into an apical and basal part by supporting cells located around the receptor cell. The basal membrane contains voltage-sensitive Ca^{2+} channels, voltage-sensitive and Ca^{2+}-activated K^+ channels, and leak channels, whereas the apical membrane contains only leak channels. The afferent nerve fiber innervates the basal membrane of the receptor cell.

The equivalent circuit model of the receptor cell is shown in Fig. 1. By using the relations $S_1 I_A = S_2 I_B$ and $\Phi_A + \Phi_B = V_{stim}$, the equation for the basal membrane potential Φ_B is represented as

$$C_0 \frac{d\Phi_B}{dt} = S_1 g_0 \left[-\Phi_B - \Phi_0 - \frac{S_2}{S_1 g_0}(I_{Ca} + I_K + I_L) + \frac{C_1}{g_0}\frac{dV_{stim}}{dt} + V_{stim} \right], \quad (1)$$

where S_1 and S_2 are the areas of apical and basal membranes, respectively; $C_0 = C_1 S_1 + C_2 S_2$; g_0 is the conductance of leak ion channels in the apical membrane; and I_{Ca}, I_K, and I_L are the ionic currents through the Ca^{2+}, K^+, and leak channels, respectively, in the basal membrane. Φ_0 is the equilibrium potential of leak channels. Detailed descriptions of these channel models appear in the previous paper (Shuai et al., 1998). The values of parameters used in Eq. 1 are listed in Table 1, which are the same values as those used in the previous paper (Shuai et al., 1998). Based on the difference in the morphology of A- and B-receptors (Szabo and Wersall, 1970; Bell et al., 1989), the values of parameters in Eq. 1 have been chosen within reasonable ranges, so that the A- and B-receptor cells respond sensitively to modulation of amplitude of V_{stim} and to that of waveform of V_{stim}, respectively (Shuai et al., 1998).

The equation determining the potential variation due to the stimuli is given for the A-cell by

$$\frac{d\Phi_B}{dt} = \frac{1}{\tau_A}\left[-\Phi_B - \Phi_0 - \frac{1}{300}(I_{Ca} + I_K + I_L) + A_{stim} \right], \quad (2)$$

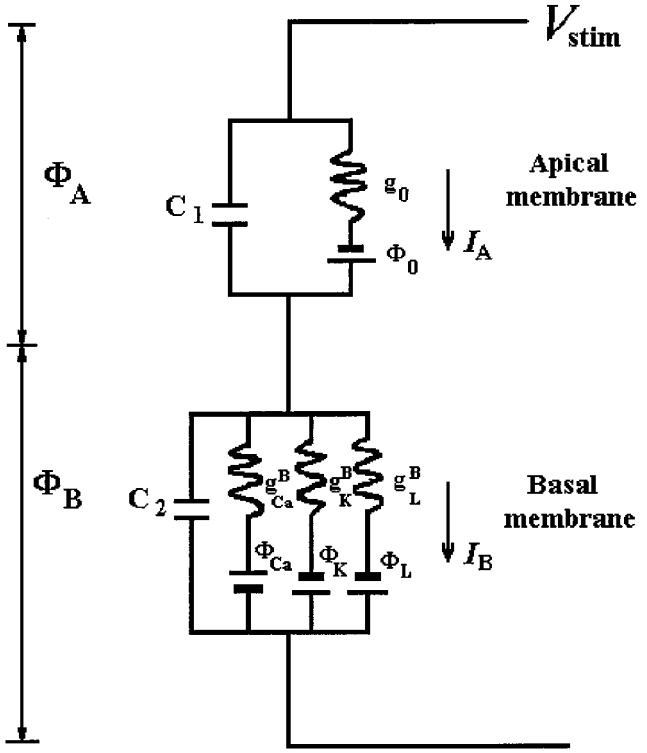

FIGURE 1 The equivalent circuit of the receptor model. Φ_A and Φ_B are the potentials of the apical and basal membranes of the cell, respectively. C_1 and C_2 are the capacitances of the unit area of apical and basal membranes, respectively. g_0 is the conductance of the leak ion channels of the unit area in the apical membrane. Φ_0 is the equilibrium potential of leak channels. g^B_{Ca}, g^B_K, and g^B_L are conductances of Ca^{2+}, K^+, and effective leak channels of the unit area in the basal membrane, respectively. Φ_{Ca}, Φ_K, and Φ_L are the equilibrium potentials of ion Ca^{2+}, K^+, and effective leak channels across the basal membrane, respectively. The arrows attached to I_A and I_B indicate the positive directions of relevant current. V_{stim} is the stimulation potential applied to the cell.

where $\tau_A = C_0/(S_1 g_0) = 1.1 \times 10^{-4}$ s, and the effective stimulus A_{stim}, which the A-cell can sense directly under application of the original stimulus V_{stim}, is represented as

$$A_{stim} = 10^{-5}\frac{dV_{stim}}{dt} + V_{stim}. \quad (3)$$

It is noted that $10^{-5}(dV_{stim}/dt)$ is of the same order of magnitude as V_{stim}, because the relationship between the maximum intensity of EOD stimulus and the maximum time variation of EOD

$$V_{stim}|_{max} \approx 1.8 \times 10^{-5} \times \left[\frac{dV_{stim}}{dt}\right]\Big|_{max} \quad (mV)$$

hold roughly for natural biphasic EODs (Shuai et al., 1998). The equation for the B-cell is given by

$$\frac{d\Phi_B}{dt} = \frac{1}{\tau_B}\left[-\Phi_B - \Phi_0 - \frac{1}{300}(I_{Ca} + I_K + I_L) + B_{stim}\right], \quad (4)$$

where $\tau_B = C_0/(S_1 g_0) = 0.92 \times 10^{-4}$ s, and the effective stimulus B_{stim} sensed by the B-cell is represented as

$$B_{stim} = \frac{25}{3} \times 10^{-5}\frac{dV_{stim}}{dt} + V_{stim}. \quad (5)$$

The functional difference between the A- and B-cells comes from the difference in the contribution of temporal variation term dV_{stim}/dt to the effective stimuli A_{stim} and B_{stim} (Shuai et al., 1998).

Spike generation in the afferent nerve fiber is induced by transmitter release, which occurs when a sufficient number of Ca^{2+} ions enter the receptor cell across the basal membrane. To calculate the impulse trains in the afferent fiber, we used the modified Hodgkin-Huxley equations (Shuai et al., 1998).

TABLE 1 Different parameter values used in Eq. 1 for the models of A- and B-cells

Cell	Parameter	Value	Unit
A-cell	$C_1 = C_2 = C_A$	3.0×10^{-2}	$\mu F/cm^2$
	S_1/S_2	0.1	
	g_0	3×10^3	$\mu S/cm^2$
	Φ_0	−70.0	mV
B-cell	$C_1 = C_2 = C_B$	2.5×10^{-3}	$\mu F/cm^2$
	S_1/S_2	10.0	
	g_0	3×10	$\mu S/cm^2$
	Φ_0	−70.0	mV

External stimuli V_{stim}

In the present study, we used three kinds of external stimuli V_{stim}, mainly for two purposes.

(i) Capacitance-distorted natural EODs

To examine the plausibility of the present models, we calculated the responses of the models to natural EODs distorted by capacitive objects. Local EODs were recorded close to the pore of an electroreceptor organ of a *G. petersii* in the presence of objects with different capacitive values from 1.2 to 50 nF (von der Emde and Bleckmann, 1992b). The p-p amplitudes of the recorded signals were normalized to a constant value. The capacitance-distorted EODs ($V_{stim}(t)$) used in the calculation were obtained from the recorded data $V^{exp}_{stim}(t)$ through the smoothing procedure,

$$V_{stim}(t) = \frac{1}{2T+1}\sum_{\tau=t-T}^{t+T} V^{exp}_{stim}(\tau), \quad (6)$$

with $T = 3$. Because the recorded signals were digitized at 2 MHz and stored in the computer, the stimulus $V_{stim}(t)$ was read out with a time step of $\delta t = 0.5 \times 10^{-6}$ s.

The capacitance-distorted EOD stimuli $V_{stim}(t)$ are shown in Fig. 2 *A* for the capacitances 1.2, 2.0, 6.0, 10.0, and 50.0 nF. As the capacitive value is increased, the first positive peak becomes larger and the second positive peak becomes smaller. The negative peak becomes more shallow, and as a

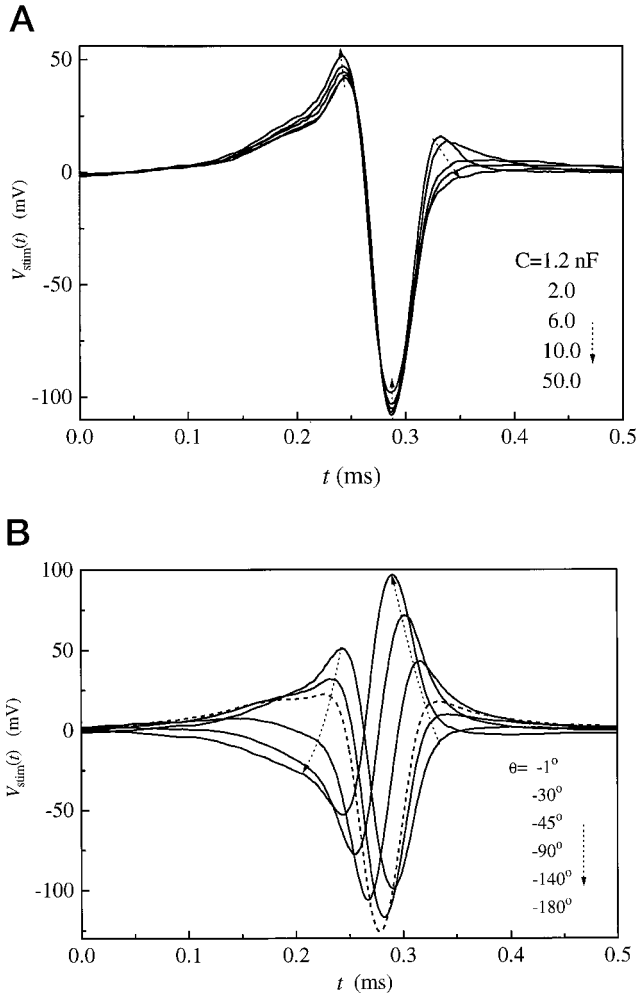

FIGURE 2 (*A*) The temporal patterns of five capacitance-distorted electric organ discharge (EOD) pulses. The dotted arrows indicate the curve order of the capacitance values from 1.2 to 2.0, 6.0, 10.0, and 50.0 nF. (*B*) The temporal patterns of six phase-shifted EOD pulses. The dotted arrows indicate the curve order of the phase angles from −1° to −30°, −45°, −90°, −140°, and −180°. The −45° phase-shifted EOD pulse is drawn with the dashed line.

result the p-p amplitude, which is the height difference between the highest positive peak and the negative peak, stays unchanged.

(ii) Phase-shifted natural EODs

To clarify the cellular origin of the inverse tuning properties of the B-receptors in contrast to A-receptors, we investigated the response properties of the A- and B-receptor models when they were stimulated with phase-shifted EODs. Von der Emde and Bleckmann (1992a,b, 1997) have used the same type of stimuli in electrophysiological experiments. To produce them, the waveform of an undistorted local EOD was altered by retarding the phase angle of all positive frequencies of the FFT phase spectrum by a constant value and by advancing the phase angle of all negative frequencies by the same angle (Heiligenberg and Altes, 1978; Hopkins and Bass, 1981; Hopkins and Westby, 1986; von der Emde and Bleckmann, 1992a,b, 1997). This method guarantees that the power spectrum and the duration of the EODs are left unchanged. We used the EODs with phase-shifted angles of −1°, −2°, −3°, −5°, −7°, −10°, −15°, −30°, −45°, −90°, −120°, −140°, and −180°. EODs without phase shifts correspond to the natural undistorted EODs, whereas EODs with a phase shift of ±180° have the inverse waveform compared to the undistorted EOD. The waveforms of EODs subjected to phase shifts between 0 and −25° are similar to waveforms of EODs distorted by capacitive objects.

The phase-shifted EOD stimuli $V_{stim}(t)$ used in the calculation were obtained by also applying the smoothing procedure given by Eq. 6 to the experimental EOD stimuli $V_{stim}^{exp}(t)$. The original data for $V_{stim}^{exp}(t)$ were recorded close to the pore of an electroreceptor organ of a *G. petersii* in the absence of any object and included many small noisy fluctuations (von der Emde and Bleckmann, 1992b). The phase-shifted EOD stimuli $V_{stim}(t)$ are shown in Fig. 2 *B,* where the phase angles used are −1°, −30°, −45°, −90°, −140°, and −180°. As the angle is increased from −1° to −180°, the first positive peak of the EOD waveform becomes smaller and the second positive peak becomes larger. At the phase shift of −45°, the height of the first peak is almost equal to that of the second peak. The negative peak becomes deeper until the angle increases up to −45°. Beyond the angle the peak becomes more shallow. However, the peak-to-peak amplitude remains almost constant.

(iii) Single-period sine wave stimuli

To investigate the time constant of the receptor models, we calculated their responses to stimulation with single-period sine wave stimuli of various frequencies. The temporal width of the stimuli was changed inversely with stimulus frequency. Because the temporal pattern of single-period sine wave is similar to the pattern of an undistorted EOD, the optimal duration of an EOD stimulus for obtaining response from A- and B-receptors has been studied experimentally by employing sine wave stimuli (Bell, 1990b; von der Emde and Bleckmann, 1992b, 1997).

RESULTS AND DISCUSSION

Responses of A- and B-receptor models to natural EODs

To clarify the cellular origin of the difference in response properties between A- and B-receptors when they are stimulated with natural EOD stimuli, we investigated the responses of the A- and B-receptor models to EOD pulses distorted by resistive and capacitive objects. We show here that the responses of A- and B-receptors stimulated with EODs distorted by resistive and capacitive objects can be explained systematically by the waveforms of the effective stimuli A_{stim} and B_{stim} defined in Eqs. 3 and 5.

Responses to resistance-distorted EODs

Pure resistive objects only alter the amplitude of the EOD stimulus: a resistance lower than that of the surrounding water leads to an increase in EOD amplitude, and a resistance higher than that of the water induces the reverse effect (Heiligenberg, 1973; von der Emde, 1990). Fig. 3 shows the calculated membrane potentials of an afferent fiber innervating a single A-receptor cell and of a fiber innervating a B-cell. The cells were stimulated by natural EODs of different amplitudes. The threshold amplitude is 8.89 mV for the A-fiber model and 4.01 mV for the B-fiber model. Also in the physiological experiment, B-fibers were found to be more sensitive than A-fibers (von der Emde and Bleckmann, 1992b). However, the threshold values obtained with the model should not be compared directly with the experimentally observed thresholds, because the definition of the

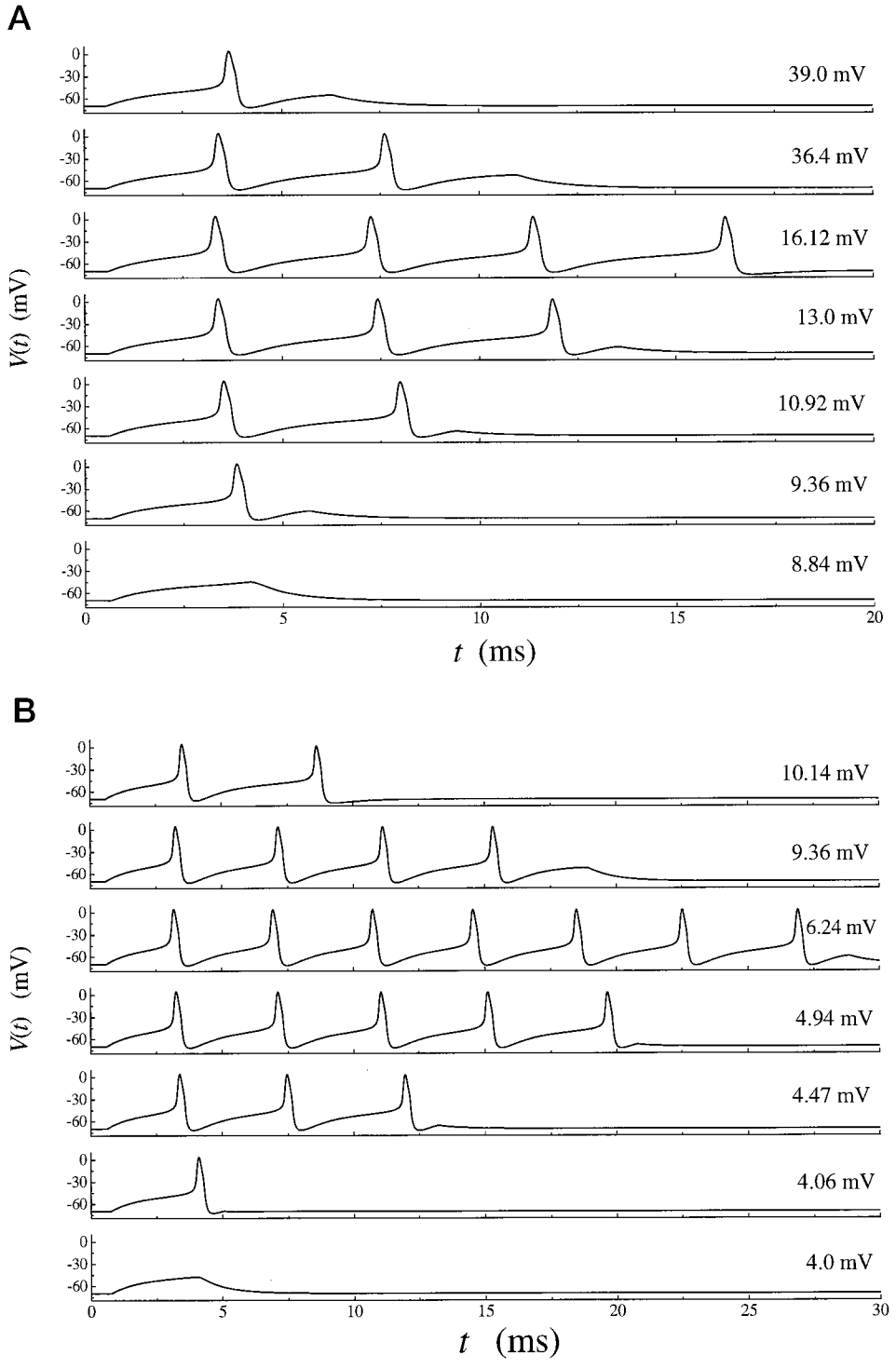

FIGURE 3 Variation of the potential $V(t)$ of the afferent fibers induced by the single undistorted EOD pulse. (*A*) Response of $V(t)$ in the A-receptor to the EOD pulses, whose amplitude values are 8.84 (below the threshold), 9.36, 10.92, 13.0, 16.12, 36.4, and 39.0 mV. (*B*) Response of $V(t)$ in the B-receptor to the EOD pulses whose amplitude values are 4.0 (below the threshold), 4.06, 4.47, 4.94, 6.24, 9.36, and 10.14 mV.

stimulus amplitude in the present model is different from that in the experiments. As described in detail in the first paper (Shuai et al., 1998), the stimulus intensity was measured as voltage drop across the cell and the skin in the experiments (Bell, 1990b; von der Emde and Bleckmann, 1992a,b). In the models, the stimulus potential was expressed as the voltage drop only across the A- or B-receptor cell. The maximum spike number is 4 and 7 for the A- and B-fibers, respectively. Very similar results were obtained in the physiological experiments (Bell, 1990b; von der Emde and Bleckmann, 1992b). The response properties of the receptor cells are similar to those stimulated by a half-period positive sinusoidal stimulus, which have been described in the previous paper (Shuai et al., 1998). The response tendencies are similar to the experimental results (Bennet, 1965; Bell, 1990b).

Fig. 4 shows the calculated values of spike latencies for the A- and B-fiber models plotted as a function of EOD amplitude. The latency of each spike decreases quickly as the EOD amplitude increases just a little above threshold. When the amplitude increases further, spike latencies first stay almost constant and then increase. This tendency also has been observed experimentally (Bell, 1990b; von der Emde and Bleckmann, 1992b).

The difference in the number of spikes induced by EOD stimulus between A- and B-receptors arises from the characteristic shapes of the effective stimuli, A_{stim} and B_{stim}, which determine directly the variation in the membrane potential as seen in Eqs. 2 and 4.

The effective stimuli A_{stim} and B_{stim}, calculated by using Eqs. 3 and 5, respectively, are shown for an undistorted EOD stimulus in Fig. 5. From Fig. 5, one can see that the effective stimulus A_{stim} is biphasic, that is, it consists of a single positive and a single negative peak. In contrast, the effective stimulus B_{stim} is triphasic, that is, it possesses one more positive peak besides the two peaks at A_{stim}. For the response property of the B-receptor, it is important that the second positive peak be higher than the first one.

The relative strength of the contributions of the positive and negative peaks determines whether the receptor cells are driven from the resting state to the exciting attraction region (see figure 3 of part I (Shuai et al., 1998)). The first positive peak of A_{stim} and B_{stim} drives the A- and B-receptor cells, respectively, to the exciting attraction region, whereas the following negative peak draws the membrane potential back toward the resting attraction region. If a second positive peaks follows, as in B_{stim}, it again drives the potential to the exciting region. Therefore, the threshold amplitude of EOD stimulus is lower for the B-cells than for the A-cells.

The U-shaped dependence of spike latencies on the EOD amplitude comes from the dynamic properties of the active conductances in the basal membrane, that is, the effective time constant of dynamic response of receptor cell with time duration of a single EOD pulse, besides the characteristic shapes of the effective stimuli, A_{stim} and B_{stim}. When the amplitude of the EOD is increased, the positive peaks become larger and the negative peak simultaneously becomes deeper. When an EOD stimulus of lower amplitude is used, the positive peak of the effective stimulus plays a dominant

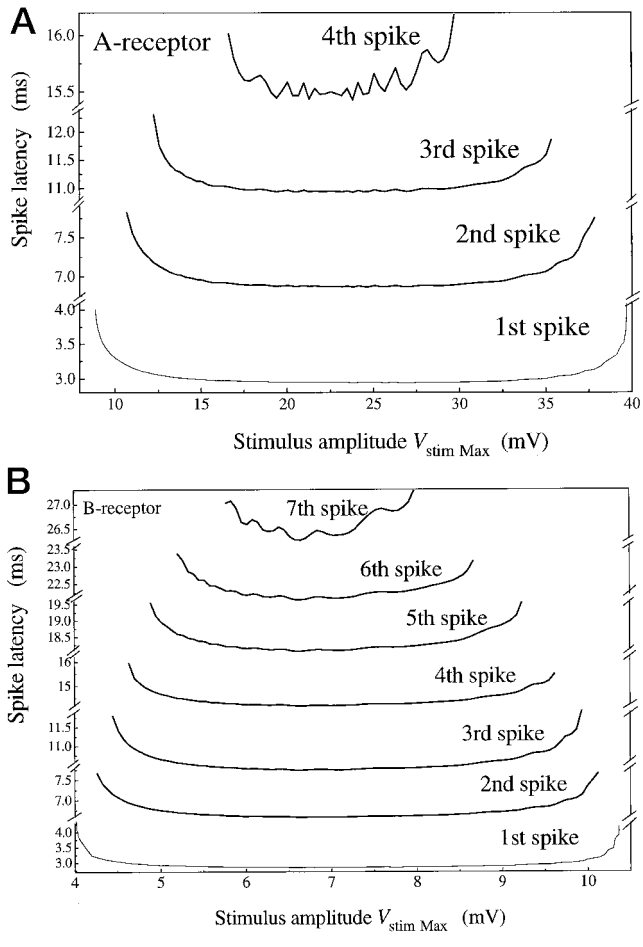

FIGURE 4 Dependence of response latency of spikes fired by the afferent fibers on the amplitude $V_{stim,Max}$ of the undistorted EOD pulse in (*A*) the A-receptor model and (*B*) the B-receptor model. This figure also shows the number of spikes induced by each EOD pulse with a different amplitude value.

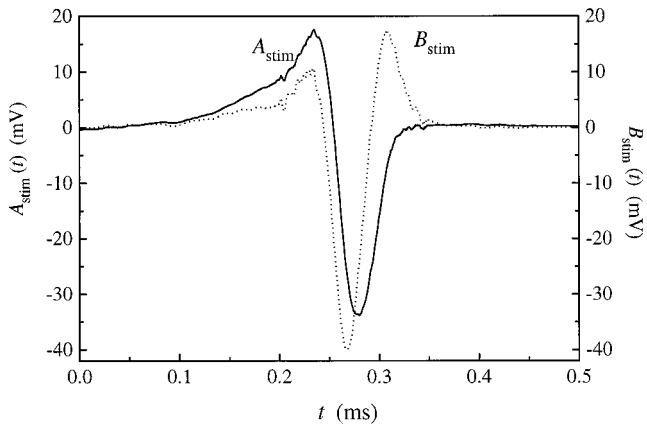

FIGURE 5 Temporal patterns of the effective stimuli $A_{stim}(t)$ (——) and $B_{stim}(t)$ (· · · · ·) affecting the A- and B-receptor cells, when they are stimulated with an undistorted EOD pulse.

role. An increase in this peak causes a decrease in spike latencies and an increase in spike number. As the stimulus amplitude increases further, the simultaneous increase in the negative peak of the effective stimulus enhances its contribution. Although the large first positive peak drives the cell to the exciting attraction region, the following strong negative peak draws it back to the resting attraction region and, furthermore, can drive it to a hyperpolarized state. Because the increasing contributions of both the positive and negative peaks are balanced within a wide range of EOD amplitude, the sensitivity of the receptors to the EOD stimuli is kept constant within a certain range. When the EOD amplitude is increased beyond this range, the magnitude of depolarization of the membrane potential induced by the first positive peak is saturated. In addition, the following large negative peak of the signal draws the membrane potential back to a hyperpolarized state. Even if, as in the case of the B-receptor model, there is a second positive peak, it is difficult to depolarize the cell from its largely hyperpolarized state back to a depolarized state. The hyperpolarization generates an increase in spike latencies and a decrease in spike number.

Responses to capacitance-distorted EODs

EODs distorted by capacitive objects with decreasing capacitive values from 100 to 1.2 nF show an increase in their waveform distortions (von der Emde, 1990) (Fig. 2 *A*). Experiments have shown that the response thresholds of A-receptors increase a little when EODs distorted by capacitances with these values are used as stimuli (von der Emde and Bleckmann, 1992a,b, 1997). When the receptors are stimulated with a set of near-threshold EODs distorted by a capacitance ranging from 100 to 2 nF, A-receptors respond with a slight increase in spike latencies and a slight decrease in spike number. A-receptors are obviously quite insensitive to the waveform distortions of an EOD stimulus. In contrast, response thresholds of B-receptors clearly decrease with decreasing capacitive values from 100 to 1.2 nF. B-receptors respond with a strong decrease in spike latencies and an increase in spike number to these stimuli (von der Emde and Bleckmann, 1992a,b, 1997). Thus they can respond positively to the EOD waveform distortion.

Fig. 6 shows the response thresholds of the A- and B-receptor models obtained, when capacitance-distorted EODs like the ones shown in Fig. 2 *A* are used as stimuli. As in the physiological experiments, thresholds are expressed as the minimum peak-to-peak (p-p) amplitude value of an EOD stimulus that can just excite the cell. The p-p amplitude thresholds for the A-receptor model increase from 26.4 to 34.7 mV, when the capacitances decrease from 50 to 1.2 nF. In contrast, the p-p amplitude thresholds of the B-receptor model decrease from 11.89 to 8.47 mV for the same capacitance range. Thus our models respond very similarly to the A- and B-receptors in the physiological experiments (von der Emde and Bleckmann, 1992a,b, 1997).

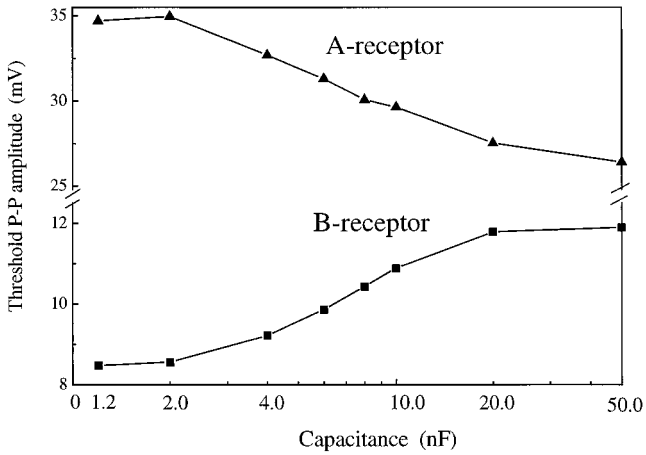

FIGURE 6 Threshold amplitudes of the capacitance-distorted EOD pulses for firing the afferent fibers in the A- and B-receptors as a function of the capacitive value of the object, which distorts the EOD waveform.

Fig. 7 shows the spike latencies of the A- and B-receptor models as a function of the threshold EOD stimuli shown in Fig. 2 *A*. The A-receptor model responds with an increase in spike latencies and a decrease in spike number when the capacitive value of the objects decreases from 50 to 1.2 nF. In contrast, the B-receptor model responds with a decrease in spike latencies and an increase in spike number, which is the opposite of the response of the A-receptors. These spike latency curves of our models look strikingly similar to the spike latency curves obtained in physiological experiments by von der Emde and Bleckmann (1992a,b, 1997).

To clarify the origin of response properties of A- and B-receptors with respect to stimulus thresholds and spike latencies, we calculated the effective stimuli A_{stim} and B_{stim} for A- and B-receptors when they are stimulated with capacitance-distorted EODs. Fig. 8, *A* and *B,* shows the effective stimuli A_{stim} and B_{stim} caused by different capacitances. The changes in the main positive and negative peaks of A_{stim} and B_{stim} are similar when the capacitance increases from 1.2 to 50 nF. However, the first positive peak is larger than the second one for the effective stimulus A_{stim}, whereas the contrary holds true for B_{stim}. Thus, when the stimulus amplitude is near the threshold, the response of the A-receptor is mainly determined by the first positive peak, whereas the response property of the B-receptor is mainly determined by the second positive peak.

Because the dominant first positive peak of A_{stim} increases with increasing capacitance (Fig. 8 *A*), the depolarization of the A-receptor is facilitated as the capacitance is increased. As a result, the threshold curves of the A-receptor decrease with an increase in capacitance of the objects. As a result, spike latencies decrease and the spike number increases. In contrast, because the dominant second positive peak of B_{stim} decreases with increasing capacitance (Fig. 8 *B*), the depolarization of the B-receptor is suppressed as the capacitance is increased. As a result, the dependencies of the threshold values, the spike latencies, and the spike

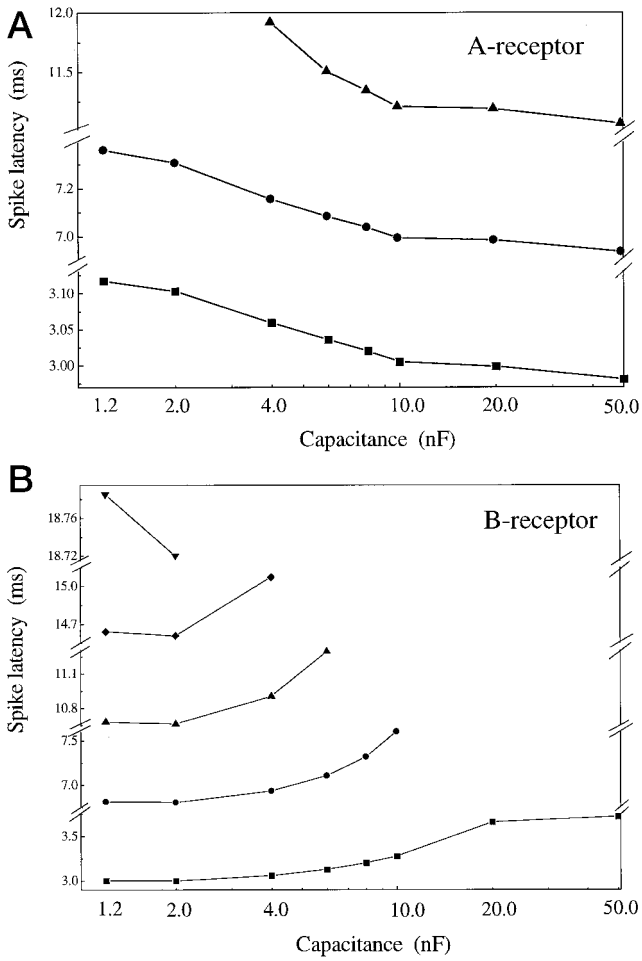

FIGURE 7 Spike latencies in the afferent fibers caused by near-threshold waveform-distorted EOD pulses induced by capacitances of various values. (*A*) Response of the A-receptor model. (*B*) Response of the B-receptor model.

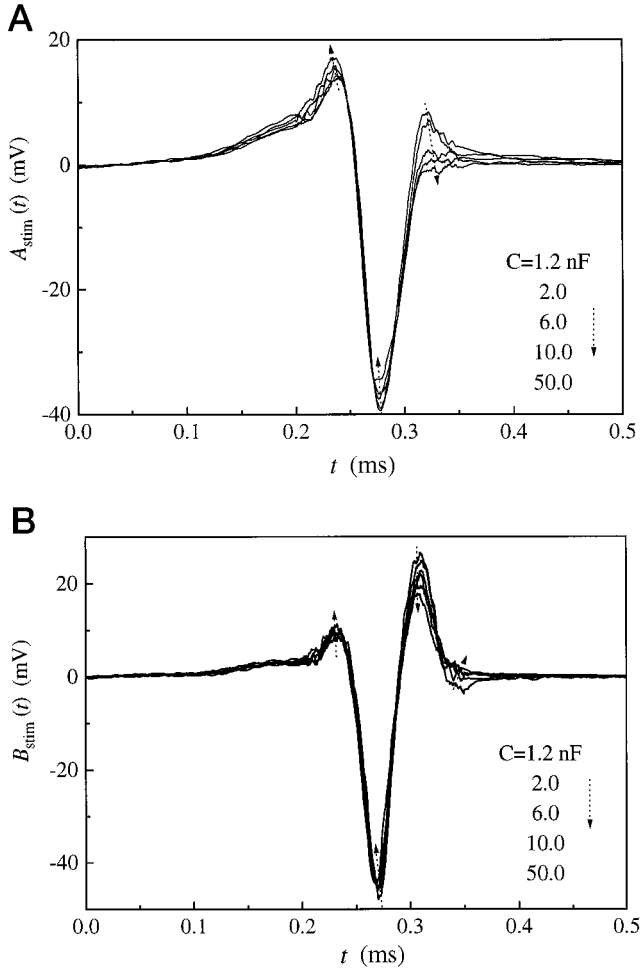

FIGURE 8 The temporal pattern of the effective stimuli, (*A*) $A_{stim}(t)$ and (*B*) $B_{stim}(t)$, influencing the A- and B-receptor cells, respectively, when stimulated by the different capacitance-distorted EOD pulses shown in Fig. 2 *A*. The dotted arrow lines indicate the order of increasing capacitance values.

number for B-receptors are opposite those for A-receptors. That is, the threshold values of B-receptors increase, the spike latencies increase, and the spike number decreases as the capacitance is increased.

Von der Emde and Bleckmann (1997) have suggested that the difference in sensitivity between A- and B-receptors does not come from a single stimulus parameter, but from the specific combination of stimulus components that occurs only in capacitance-distorted EODs. The results obtained with our models suggest that both A- and B-receptors are sensitive to the effective stimuli A_{stim} and B_{stim}, which consist of the specific combination of V_{stim} and dV_{stim}/dt, as obtained from Eqs. 3 and 5.

Cellular origin of inverse waveform tuning

Von der Emde and Bleckmann (1997) have shown that both A- and B-receptors are inversely waveform tuned, that is, they respond more sensitively to the 180° inverted EOD waveform than to the undistorted EOD. By shifting the phases of the fast Fourier transform (FFT) phase spectrum of an undistorted EOD pulse, it is possible to mimic the waveform distortions occurring in the presence of capacitance objects (Heiligenberg and Altes, 1978; Hopkins and Bass, 1981; Hopkins and Westby, 1986; von der Emde and Bleckmann, 1992b). These phase-shifted EODs have constant p-p amplitude spectra. Small negative phase shifts between −1° and −20° cause waveform distortions similar to those induced by capacitive objects. Employing such phase-shifted signals, it was demonstrated experimentally that B-receptors but not A-receptors are extremely sensitive to waveform distortions in the natural range (von der Emde and Bleckmann, 1992a,b, 1997). B-receptors even respond to a phase shift of only −1°. A-receptors, on the other hand, change their firing behavior only a little when phase shifts up to −20° are used. It is not yet clear what the microscopic origin of the inverse waveform tuning is.

In this study, we investigated the properties of the responses of A- and B-receptor models to the phase-shifted EODs to clarify the cellular origin of the inverse waveform

tuning. The sensitivity of the receptors to the phase-shifted EODs is caused mainly by two factors. One is how the waveform of effective stimuli A_{stim} and B_{stim} is changed depending on the phase shift of EOD. The other is the time constant of dynamical variation of receptor membrane potential, that is, the time duration during which the receptor can respond to a single continuous stimulus.

We consider at first the effects of the two factors, one after the other.

Properties of responses of A- and B-receptor models to phase-shifted EODs

Fig. 9 shows the response thresholds of A- and B-receptor models to the phase-shifted EODs whose waveforms are shown in Fig. 2 *B*. Threshold is again expressed as the p-p amplitude value of an EOD stimulus that can just evoke a spike response of the afferent fiber. The threshold p-p amplitude values of the A-receptor model increase from 26.1 to 38.25 mV when the phase angle increases from −1° to −45°, and then decreases to 17.25 mV with a further change to −180°. In contrast, in the B-receptor model, thresholds decrease constantly from 11.85 to 4.5 mV with increasing phase angles from 0 to −180°. Our results indicate that both A- and B-receptors have their minimum thresholds at −180°, that is, they are inversely waveform tuned. Thus the models reproduce qualitatively the experimental results of von der Emde and Bleckmann (1992b, 1997). Even though the simulation results for the A-receptor model differ somewhat from the experimental results, the general tendency is the same.

The inverse tuning properties are also seen when spike latencies are plotted versus phase shift. Fig. 10, *A* and *B,* shows the latency response curves for the A- and B-receptor models for stimulus amplitude just a little above the threshold. Spike latencies and the number of spikes depend on the angle of the phase shift. The response properties of the models agree quite well with the experimental results (von der Emde and Bleckmann, 1992b).

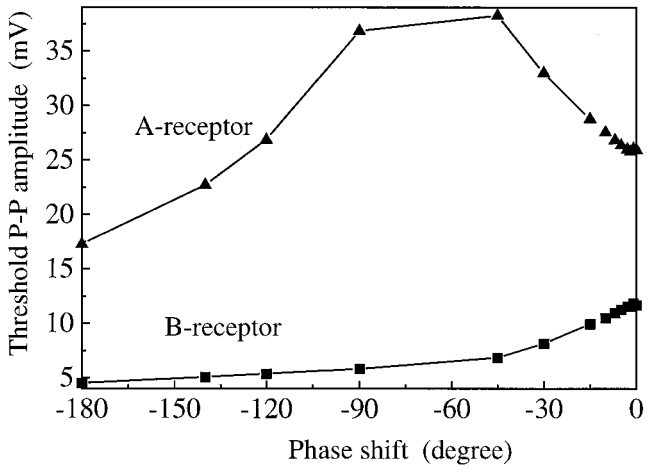

FIGURE 9 Amplitude thresholds (p-p amplitude) of the A- and B-receptor models for phase-shifted EOD pulses. Phase shift angles were varied between −180° to 0°.

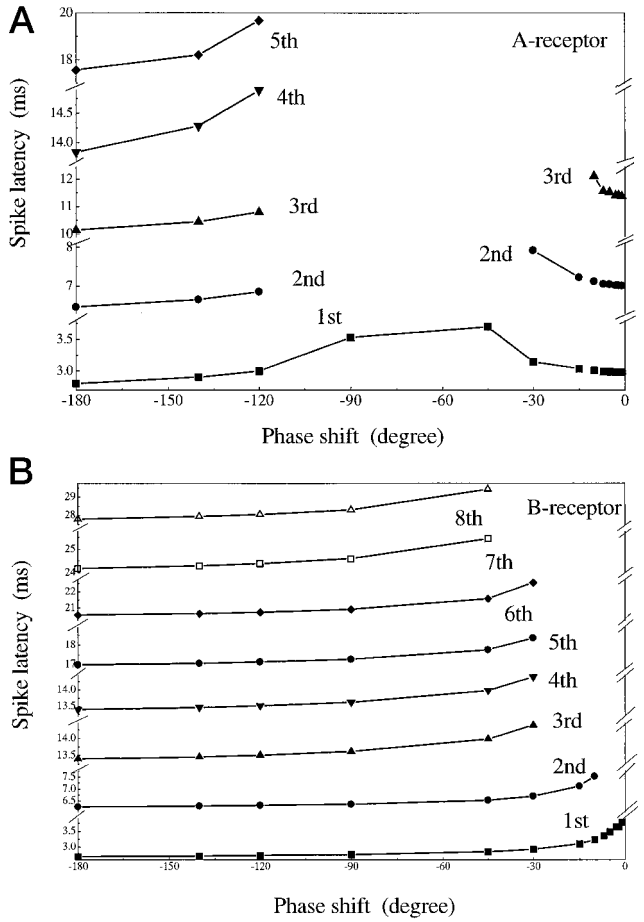

FIGURE 10 Spike latency response curves of (*A*) the A-receptor model and (*B*) the B-receptor model for a set of phase-shifted EODs with a fixed p-p amplitude. The value of the fixed amplitude is 39.0 mV for the A-receptor and 11.9 mV for the B-receptor.

To clarify the mechanism of the inverse waveform tuning, we calculated the effective stimuli, A_{stim} and B_{stim}, for the A- and B-receptor models, using the phase-shifted EODs shown in Fig. 2 *B*. Fig. 11 shows the temporal variation patterns of the effective stimuli. It can be seen that with increasing phase angle, the first positive peak of the stimuli decreases, whereas the second one increases in both A_{stim} and B_{stim}. The negative peak becomes more negative with increasing phase-shifts from −1° to −45° and then increases with an increase in phase angle from −45° to −180°. In the stimuli A_{stim}, the first positive peak is larger than the second one for the phase shifts from −1° to −45°. For the −45° phase-shifted stimulus, which is shown as the dotted line in Fig. 11, the two positive peaks of A_{stim} are almost equal in their amplitudes. For even larger phase shifts, the second positive peak becomes larger than the first one. In the stimulus B_{stim}, the second positive peak is larger than the first one, independently of the angle of phase shift (Fig. 11 *B*).

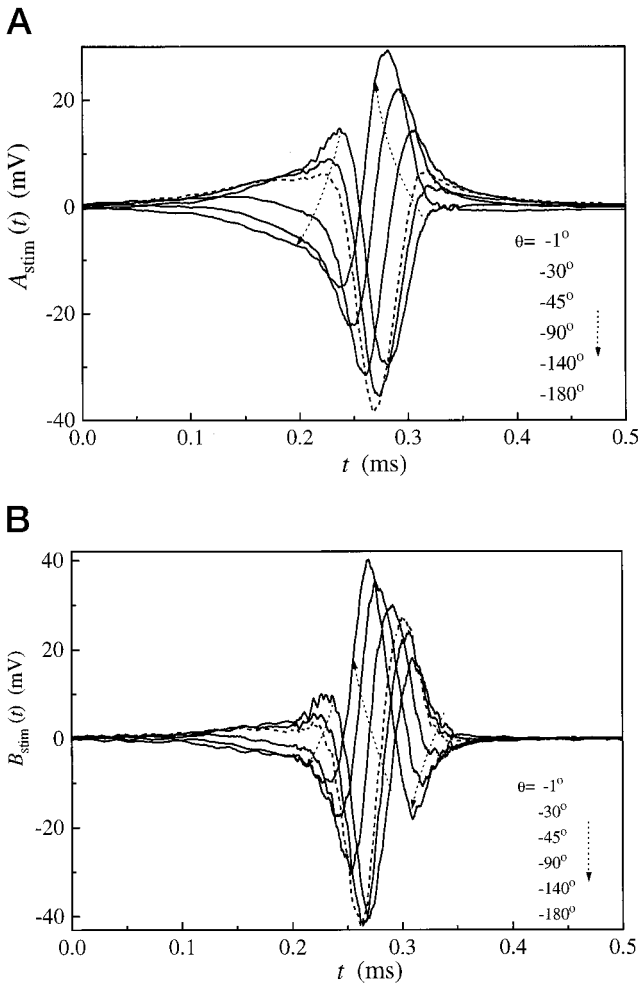

FIGURE 11 The temporal patterns of the effective stimuli, (*A*) $A_{stim}(t)$ and (*B*) $B_{stim}(t)$, influencing the A- and B-receptor cells when they are stimulated with the six phase-shifted EOD pulses shown in Fig. 2 *B*. The waveform of a stimulus phase shifted by −45° is drawn as a dashed line. The dotted arrow lines indicate the order of increasing phase angle.

The threshold and latency dependencies on the phase angles in both receptor types can be explained based on the change in the effective stimuli induced by an EOD phase shift. The properties of the responses of both the A- and B-receptor models to the phase-shifted EODs are mainly determined by the maximum positive peak of the effective stimuli. In the A-receptor model, the p-p amplitude threshold values and the first spike latency increase because the first positive peak, which is larger than the second one, decreases when the phase angle changes from −1° to −45°. Threshold values and spike latencies decrease with a change in the phase angle from −45° to −180° because of the second positive peak of the effective stimuli, which becomes larger than the first one between −45° and −180°. The p-p amplitude threshold values and the spike latencies of the B-receptor model decrease monotonically with changing phase angle from −1° to −180° because the second positive peak, which is always larger than the first one, increases with the phase change. The inverse waveform tuning is obtained in both receptor models, because among phase-shifted EODs the ±180° phase-shifted EODs have the maximum positive peak and the minimum negative peak (Fig. 11).

Temporal width of EOD pulse stimuli for optimal response sensitivity

For the inverse tuning property of the receptor cells, it is quite important how long the time constants of response dynamics of the receptors are. Only when the time constant is on the order of the time duration of an EOD pulse the receptors can sense clearly the whole temporal pattern of the EOD pulses, which consists of a first positive, a negative, and a second positive peak. If the time constant is much shorter than the pulse width, the receptor can sense only the first positive peak.

The optimal time duration of an EOD for the receptors has been studied experimentally by using the single-period sine wave stimuli (Bell, 1990b; von der Emde and Bleckmann, 1992b, 1997). Because the temporal pattern of single-period sine wave stimuli is very similar to the biphasic pattern of an undistorted EOD pulse, the sine wave stimuli have been used to investigate the best temporal width (duration) of the stimuli for the response sensitivity of A- and B-receptors.

Bell (1990b) measured the dependence of threshold amplitude of a sine wave stimuli on the frequency (the reciprocal of the temporal width). A-receptors showed a great deal more variability than B-receptors in both the shapes of the threshold curves and in the mean threshold values. Whereas the minimum thresholds of individual A-receptors were distributed widely at frequencies between 100 and 2000 Hz, all B-receptors had minimum thresholds around 100–200 Hz for both initially positive and initially negative stimuli. Because mormyromast receptors are inversely waveform tuned, the thresholds were a little higher for initially positive sine wave stimuli compared to initially negative sine waves. Interestingly, this difference between the two stimulus types increased substantially at frequencies below 100 Hz (Bell, 1990b).

To investigate how long the response time constants of the A- and B-receptor models are, we calculated the threshold values for various frequency values of sine wave stimuli. Fig. 12 shows the threshold curves of the models for the initially positive and initially negative sine wave stimuli. The threshold value at each frequency is higher in the A-receptor model than in the B-receptor model, as obtained experimentally. In the case in which the stimuli are initially positive sine wave, the A- and B-receptor models have their minima at the frequency of 1100 Hz and 900 Hz, respectively. In the case of initially negative sine wave stimuli, the threshold minima occur at 400 Hz in the A-receptor and at 460 Hz in the B-receptor. That is, the optimal time width of the former stimuli is around 1 ms for both the A- and B-receptor types, whereas the width of the latter stimuli is

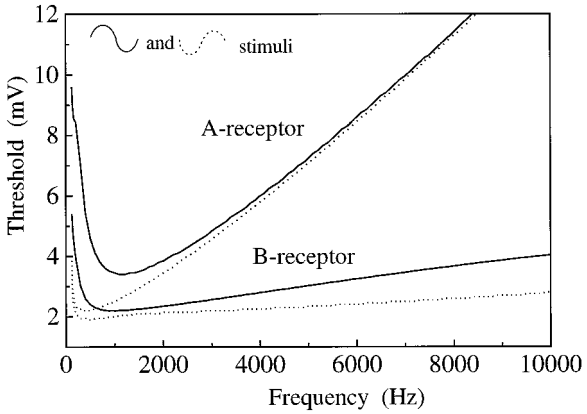

FIGURE 12 Threshold amplitudes of the A- and B-receptor models when they are stimulated with single-period sine wave stimuli of different frequencies. Solid curves and dotted curves represent the threshold values for the initially positive and negative sine waves, respectively.

around 2 ms for both of the receptors. As in the physiological experiments, both the A- and B-receptor models have a lower threshold in the case of a sine wave with an initial negative polarity than in the case of an initial positive polarity. This difference in the threshold for initially positive or initially negative stimuli increases noticeably in the A-receptor model at lower stimulus frequencies, as observed by Bell (1990b).

Von der Emde and Bleckmann (1992b) used a somewhat different method to analyze experimentally the frequency tuning property of mormyromasts. Stimuli with amplitudes just a little bit above threshold were applied and spike latencies in the afferent fibers were recorded. It turned out that minimum spike latencies and maximum spike numbers were found at an average frequency of 2.0 kHz in A-receptors and at 2.1 kHz in B-receptors.

The present models of A- and B-receptors have very similar optimal frequencies. Fig. 13, *A* and *B,* shows the simulation results of spike latencies of A- and B-receptors for initially positive sine wave stimuli. In the A-receptor model, the minimum first spike latency occurs at a stimulus frequency of 2050 Hz with a stimulus amplitude of 5.2 mV. The B-receptor model has the minimum spike latency at the frequency of 2150 Hz with a stimulus amplitude of 2.6 mV. The calculated values agree quite well with the experimental results (von der Emde and Bleckmann, 1992b). The optimal temporal width of the stimulus is 0.5 ms for both the A- and B-receptors.

The values of optimal temporal width of single sine wave stimuli are in the range of 0.5–2 ms. The frequency tuning of the receptors is not so sharp (Figs. 12 and 13) that the time constant of receptor response dynamics can be definitely estimated based on the results. However, because the temporal width of natural EOD pulses is ~0.3 ms (Fig. 2), it seems quite possible that the receptor models clearly sense the whole temporal pattern of a natural EOD pulse.

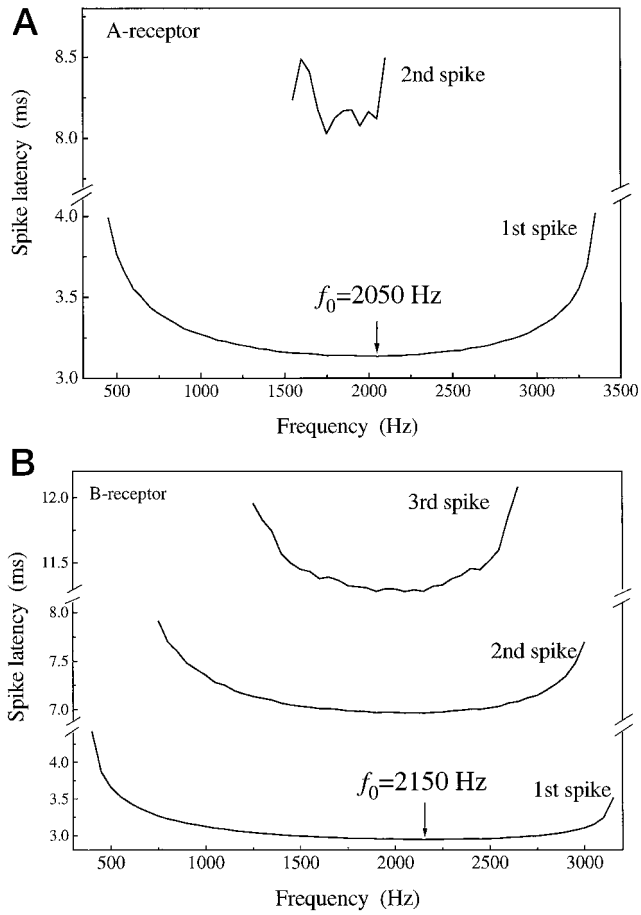

FIGURE 13 Spike latencies induced by the initially positive sine wave pulses of different frequencies. (*A*) Responses of the A-receptor model to the sine wave of a fixed amplitude of 5.5 mV. The minimum latency occurs at an optimum frequency of 2050 Hz. (*B*) Responses of the B-receptor model to the sine wave of a fixed amplitude of 2.5 mV. The minimum spike latency occurs at an optimal frequency of 2150 Hz.

Effect of object resistance on the response to object capacitance

Capacitive objects modify both the waveform and the amplitude of EODs, as shown in Fig. 2 *A.* Pure resistive objects, on the other hand, alter only the EOD amplitude. However, natural objects usually have complex impedances consisting of various combinations of resistance and capacitance. Therefore, it is interesting to investigate how the properties of the responses of the receptors to the capacitive-distorted EODs are influenced by difference in EOD amplitudes.

Fig. 14, *A* and *B,* shows first spike latencies of A- and B-receptor models as a function of capacitance value for different overall stimulus amplitude. In A-receptors, capacitance-distorted EODs at threshold amplitude cause first spike latencies to decrease, as shown in Fig. 7 *A,* when the value of the capacitance increases. A similar dependency exists for most EOD amplitudes, except for EODs of medium amplitude (*curve C,* Fig. 14 *A*). The latency curves for

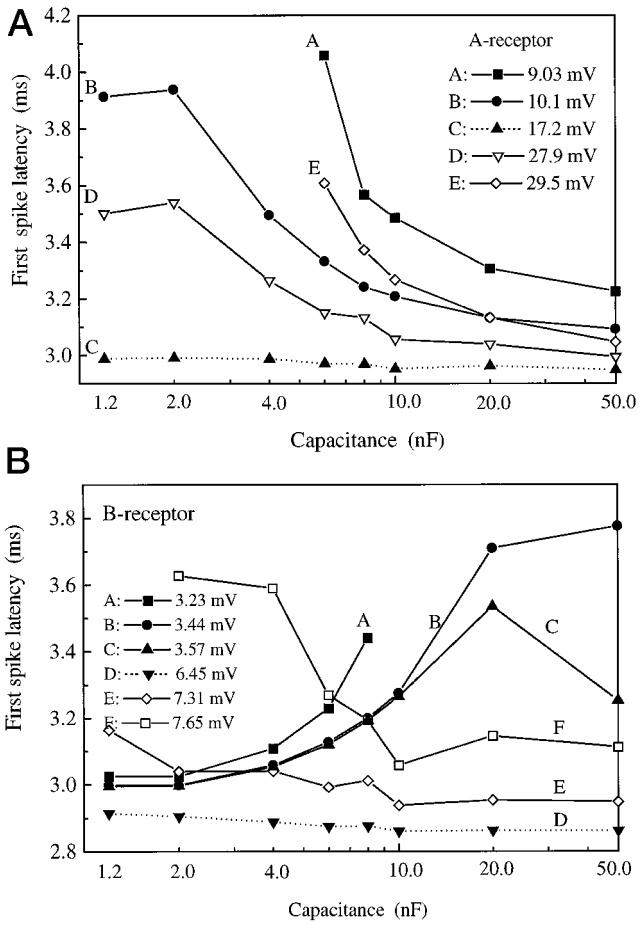

FIGURE 14 First spike latencies of the receptor models stimulated by capacitance-distorted EODs of different fixed amplitudes. (*A*) Responses of the A-receptor model. (*B*) Responses of the B-receptor model.

EODs with a medium amplitude are almost independent of the capacitance value.

These results can be understood based on the variations of effective stimulus A_{stim} influencing the A-receptor and the effective time constant of dynamic response of the receptor cell. As the amplitude of the capacitance-distorted EODs is increased, A_{stim} has a large first positive peak and a small negative peak. At lower amplitudes, the response of the A-receptor is mainly determined by the first positive peak. Because the first positive peak increases with an increase in stimulus amplitude, the depolarization of the A-receptor is facilitated. As a result, the first spike latency decreases, as seen in the amplitude change A $\rightarrow$ B $\rightarrow$ C in Fig. 14 *A*. At medium amplitudes, the response stays in the saturation state because the depolarization effect due to the first positive peak is balanced by the hyperpolarization effect due to the negative peak (*curve C*). At high stimulus amplitude, the contribution of the negative peak becomes larger and, as a result, the first spike latency increases again (*curves D and E*).

The response properties of the B-receptor model shown in Fig. 14 *B* are more complex. When the amplitude of the stimulus is just above the threshold, first spike latencies increase with increasing capacitance (*curves A* and *B* in Fig. 14 *B*). If the stimulus amplitude is a little higher, first spike latency first increases and then decreases with increasing capacitance values (*curve C*). For medium stimulus amplitudes, an almost constant first spike latency is observed over a range of capacitance from 1.2 to 50 nF (*curve D*). If the stimulus amplitude is well above threshold, an opposite dependence of first spike latency on capacitance value is observed: a decrease in spike latencies occurs with an increase in capacitance value (*curves E* and *F*).

These response properties of B-receptors can also be explained by the changes in effective stimuli B_{stim} and the effective time constant of dynamic response of the receptor cell. At low amplitudes, the response is mainly determined by the second positive peak of the stimulus, as seen in Fig. 8 *B*. Because the second positive peak increases with an increase in the stimulus amplitude, first spike latency decreases, as seen from curves A and B in Fig. 14 *B*. In the case of a medium amplitude, the depolarization effect due to the second positive peak is balanced by the hyperpolarization effect due to the negative peak. As a result, the receptor stays in the saturation state (*curve D*). At high stimulus amplitude, first spike latencies increase because of the increase in the negative peak, which suppresses the depolarization of the B-cell (*curves E* and *F*).

In addition, one can see in Fig. 14 *B* that the dependency of the first spike latency on capacitance value is reversed as the stimulus amplitude increases (*curves A, B, C,* $\rightarrow D \rightarrow E$, *F*). Moreover, this reversal can be explained by a change in B_{stim}. At lower amplitudes, the second positive peak of B_{stim}, which mainly determines the receptor response, decreases with an increase in capacitance value. As a result, first spike latencies increase when the capacitance increases from 1.2 to 50 nF (*curves A* and *B* in Fig. 14 *B*). When stimulus amplitude is higher, the negative peak of the stimulus contributes more strongly to the receptor response. This is so because at high amplitude, the size of the negative peak becomes smaller and the first positive peak increases with increasing capacitance. It follows that the depolarization of B-receptor is more facilitated when the capacitance value increases. As a result, the B-receptor model behavior at high stimulus amplitudes is the opposite of its behavior at low amplitudes.

CONCLUDING REMARKS

First, based on the present model, we consider the cellular factors that mainly determine the time constant of receptor response dynamics. Second, we discuss briefly the relationship between stimulus amplitude and various response properties of natural and model electroreceptors.

Factor determining the receptor time constant

First, we considered the relationship of the time constant τ_e and the optimal frequency ω_0 of a sine wave stimulus in a

simplified model of receptor membrane potential $\phi(t)$. The potential $\phi(t)$ is determined in this simplified model by

$$\frac{d\phi(t)}{dt} = -\frac{1}{\tau_e}\phi(t) + a\frac{dV_{stim}}{dt} + bV_{stim}, \quad (7)$$

$$V_{stim} = \sin \omega t, \quad (8)$$

where τ_e is the effective time constant of the receptor cell, and a and b are constant parameters. The steady-state solution of Eq. 7 is

$$\phi(t) = C(\omega)\cos \omega t + S(\omega)\sin \omega t, \quad (9)$$

where the amplitudes $C(\omega)$ and $S(\omega)$ are given by

$$C(\omega) = \frac{(a - b\tau_e)\tau_e\omega}{1 + \tau_e^2\omega^2}, \quad S(\omega) = a + \frac{b\tau_e - a}{1 + \tau_e^2\omega^2}. \quad (10)$$

The absolute value of amplitude, $|C(\omega)|$, becomes maximum at $\omega=1/\tau_e$, but $|S(\omega)|$ does not depend sensitively on ω. Therefore, the optimal frequency ω_0 for the simplified model is nearly equal to the reciprocal of the effective time constant τ_e.

Second, we considered what factors determine the effective time constant τ_e in the A- and B-receptor models. We compare Eq. 1 with Eq. 7 and use the representations of I_{Ca}, I_K, and I_L (Shuai et al., 1998),

$$I_{Ca} = g_{Ca}^B(\Phi_B - \Phi_{Ca}), \quad (11)$$

$$I_K = g_K^B(\Phi_B - \Phi_K),$$

$$I_L = g_L^B(\Phi_B - \Phi_L).$$

We obtained the expression of τ_e as

$$\tau_e = \frac{S_1C_1 + S_2C_2}{S_1g_0 + S_2(g_{Ca}^B + g_K^B + g_L^B)}, \quad (12)$$

where g_{Ca}^B, g_K^B, and g_L^B are the conductance of Ca^{2+} channels, Ca^{2+}-activated K^+ channels, and leak ion channels in the basal membrane, respectively. The conductances g_0 and g_L^B are constant, but g_{Ca}^B and g_K^B change nonlinearly with varying basal membrane potential Φ_B (Shuai et al., 1998). Thus the effective time constant τ_e and the optimal frequency ω_0 are changed with an increase in the stimulus amplitude.

The optimal frequency ω_0 ($\simeq 1/\tau_e$) of the A-receptor is very close to the frequency of the B-receptor in the case in which the stimulus amplitude is near threshold for firing of the afferent fiber, as shown in Figs. 12 and 13. The magnitude of depolarization ($\Delta\Phi_B$) is determined mainly by the nonlinear conduction part S_2 (I_{Ca} + I_K) in Eq. 1. The magnitude ($\Delta\Phi_B$) induced by the relevant threshold stimulus for the A-receptor is equivalent to that for the B-receptor. Therefore, the value of $S_2(g_{Ca}^B + g_K^B)/C_0$ in the A-receptor is nearly equal to the value in the B-receptor.

Relation of the amplitude "effect" to experimental results

It is one of the noticeable results obtained in the present study that the responses of A- and B-receptors to EODs change qualitatively, depending on the magnitude of stimulus amplitude. We call this the "amplitude effect." We could show the amplitude effects for the spike latencies induced by undistorted EOD stimuli as shown in Figs. 3 and 4, and for the dependence of receptor response to different capacitive object properties on stimulus amplitude (Fig. 14).

The amplitude effects in the regions of low and medium stimulus amplitudes were also observed in physiological experiments (Bell, 1990b; von der Emde and Bleckmann, 1992b, 1997). It has also been shown that as in Fig. 4, receptor responses of both A- and B-receptors decrease, i.e., spike latencies increase and spike numbers decrease, when stimulated with undistorted EODs with very high-stimulus amplitudes (Bell, 1990b; von der Emde and Bleckmann, 1992b). However, the dependency of the properties of the receptor to capacitive objects in the high-amplitude range has not been observed experimentally.

REFERENCES

Bastian, J. 1986. Electrolocation: behavior, anatomy and physiology. *In* Electroreception. T. H. Bullock and W. Heiligenberg, editors. John-Wiley and Sons, New York. 577–612.

Bell, C. C. 1990a. Mormyromast electroreceptor organs and their afferent fibers in mormyrid fish. II. Intra-axonal recordings show initial stages of central processing. *J. Neurophysiol.* 63:303–318.

Bell, C. C. 1990b. Mormyromast electroreceptor organs and their afferent fibers in mormyrid fish. III. Physiological differences between two morphological types of fibers. *J. Neurophysiol.* 63:319–332.

Bell, C. C., H. Zakon, and T. E. Finger. 1989. Mormyromast electroreceptor organs and their afferent fibers in mormyrid fish. I. Morphology. *J. Comp. Neurol.* 286:391–407.

Bennet, M. V. L. 1965. Electroreceptors in mormyrids. *Cold Spring Harb. Symp. Quant. Biol.* 30:245–262.

Hall, C., C. C. Bell, and R. Zelick. 1995. Behavioral evidence of a latency code for stimulus intensity in mormyrid electric fish. *J. Comp. Physiol. A.* 177:29–39.

Heiligenberg, W. 1973. Electrolocation of objects in the electric fish *Eigenmannia. J. Comp. Physiol.* 87:137–164.

Heiligenberg, W., and R. A. Altes. 1978. Phase sensitivity in electroreception. *Science* 199:1001–1004.

Hopkins, C. D., and A. H. Bass. 1981. Temporal coding of species recognition signals in an electric fish. *Science.* 212:85–87.

Hopkins, C. D., and G. W. M. Westby. 1986. Time domain processing of electric organ discharges by pulse-type electric fish. *Brain Behav. Evol.* 29:77–104.

Shuai, J. W., Y. Kashimori, and T. Kambara. 1998. Electroreceptor model of weakly electric fish *G. Petersii.* I: The model and the origin of differences between A- and B-receptors. *Biophys. J.* 75:1712–1726.

Szabo, T., and S. Hagiwara. 1967. A latency-change mechanism involved in sensory coding of electric fish (mormyrids). *Physiol. Behav.* 2:331–335.

Szabo, T., and J. Wersall. 1970. Ultrastructure of an electroreceptor (mormyromast) in a mormyrid fish, *Gnathnemus petersii. J. Ultrastruct. Res.* 30:473–490.

von der Emde, G. 1990. Discrimination of objects through electrolocation in the weakly electric fish, *Gnathonemus petersii. J. Comp. Physiol. A.* 167:413–421.

von der Emde, G. 1993. Capacitance discrimination in electrolocating, weakly electric pulse fish. *Naturwissenschaften* 80:231–233.

von der Emde, G., and C. C. Bell. 1994. Responses of cells in the mormyrid electrosensory lobe to EODs with distorted waveforms: implications for capacitance detection. *J. Comp. Physiol. A.* 175:83–93.

von der Emde, G., and H. Bleckmann. 1992a. Extreme phase sensitivity of afferents which innervate mormyromast electroreceptors. *Naturwissenschaften* 79:131–133.

von der Emde, G., and H. Bleckmann. 1992b. Differential response of two types of electroreceptive afferents to signal distortions may permit capacitance measurement in a weakly electric fish, *Gnathonemus petersii. J. Comp. Physiol. A.* 171:683–694.

von der Emde, G., and H. Bleckmann. 1997. Waveform tuning of electroreceptor cells in the weakly electric fish, *Gnathonemus petersii. J. Comp. Physiol. A.* 181:511–524.

von der Emde, G., and B. Ronacher. 1994. Perception of electric properties of objects in electrolocating weakly electric fish: two-dimensional similarity scaling reveals a city-block metric. *J. Comp. Physiol. A.* 175: 801–812.